International Journal of Applied Science; Vol. 1, No. 2; 2018
ISSN 2576-7240 E-ISSN 2576-7259
https://doi.org/10.30560/ijas.v1n2p6

Circuit Optimization for Enhancing the Output Power of a Piezoelectric Energy Harvester

Anahita Zargarani[1] & S. Nima Mahmoodi[1]

[1] Department of Mechanical Engineering, The University of Alabama, Tuscaloosa, AL 35487, USA

Correspondence: S. Nima Mahmoodi, Department of Mechanical Engineering, The University of Alabama, Tuscaloosa, AL 35487, USA. Tel: 1-205-348-5056. E-mail: nmahmoodi@eng.ua.edu

Received: June 2, 2018; Accepted: July 3, 2018; Published: August 29, 2018

Abstract

In this paper, a new method is proposed for improving a piezoelectric energy harvester's output power. A piezoelectric vibration energy harvester has an inherent internal capacitance. The new approach adopts inductance to reduce the reactance of the internal capacitance and enhance the output power. To show the practicality of this method, four electrical circuits are investigated numerically and experimentally for a piezoelectric beam energy harvester: Simple Resistive Load, Inductive Load, standard AC-DC, and Inductive AC-DC circuits. An Inductive Load circuit is built by adding an inductor to a Simple Resistive Load circuit, while an Inductive AC-DC circuit is built by adding an inductor to a standard AC-DC circuit. Experimental results indicate that the Inductive Load and the Inductive AC-DC circuits avail the Simple Resistive Load and standard AC-DC circuits respectively. The inductive AC-DC circuit shows a 6.7% increase in the output power compared to the standard AC-DC circuit.

Keywords: vibration, energy harvesting, piezoelectric, inductive power conditioning circuit

1. Introduction

The need for electronic devices that are self-powered has created a lot of interest for research in the field of energy harvesting (Sodano, Inman, & Park, 2005a). Such devices are desirable in manufacturing as they allow for mounting in remote areas, where it is costly to maintain. For instance, finite supplies such as batteries require replacement periodically, which can be difficult and tedious if it is located deep within a manufacturing assembly. Therefore, power harvesting seems to be very useful for generating such small amounts of power often necessary for such devices (Ju et al., 2013).

There are different methods for energy harvesting; namely, solar power (Fröhlich, Bezerra, & Slongo, 2014), thermal energy (Monfray et al., 2012; Niotaki, Georgiadis, & Collado, 2013), and vibration energy harvesting. Some of the most common methods are those that convert mechanical vibrations surrounding a system into electrical energy, which have many applications including use in the transportation industry (Nuffer & Bein, 2006), wearable devices (Zhao & You, 2014), and MEMS (Korayem & Omidi, 2012; Omidi, Korayem, & Korayem, 2013). This is due to the fact that vibration energy exists in any dynamic system (Priya & Inman, 2009) including bridges (Baldwin, Roswurm, Nolan, & Holliday, 2011), (Peigney & Siegert, 2013) human bodies (De Pasquale & Soma, 2013), etc. Similarly, there are different methods used for conversion of vibration energy to electrical energy; namely, piezoelectric, electromagnetic (Hadas, Kluge, Singule, & Ondrusek, 2007), electrostatic (Choi, Han, Kim, & Yoon, 2011), and capacitive transducers (Roundy, Wright, & Rabaey, 2003). Piezoelectric-based vibration energy harvesting is a commonly used approach among the aforementioned methods (Priya & Inman, 2009), as piezoelectric materials not only have stronger electromechanical coupling but they also do not demand an external voltage source (I. Lien, Shu, Wu, Shiu, & Lin, 2010). Piezoelectric materials come in the following types: Lead Zirconate Titanate (PZT) materials (Hatti et al., 2011; Xu et al., 2013), Polyvinylidene flouride (PVDF) films (Frey, Carmichael, Kavanaugh, & Mahmoodi, 2014; Kodali, Mahidhar, Lokesh, Prasad, & Sambandan, 2012; Zargarani & Mahmoodi, 2015), Macro Fiber Composites (MFCs) (Ju et al., 2013), and relaxor ferroelectrics (Wang, Sun, & Qin, 2008). There have been an extensive number of studies testing these materials on common structures such as cantilever beams (Erturk & Inman, 2008) and flags (Frey et al., 2014; Wynn, Truitt, Heim, & Mahmoodi, 2013; Zargarani & Mahmoodi, 2015).

The three main components of piezoelectric-based vibration energy harvesting systems are a piezoelectric harvester, an oscillatory system, and an electrical interface. An oscillator is used to shake the piezoelectric such that it represents the vibration surrounding dynamic systems (I. Lien et al., 2010). The electrical circuit is utilized

to enhance and/or store the voltage produced by the piezoelectric harvester. As mentioned, an electrical interface is one of the major components of a piezoelectric-based energy harvesting system. Thus, a large number of researchers have been studying different electrical interfaces for storing (Sodano, Inman, & Park, 2005b) and/or optimizing the output power (Hui-yu Li, Hua Li, & Horn-sen Tzou, 2011; Ottman, Hofmann, Bhatt, & Lesieutre, 2002) of piezoelectric-based energy harvesters. The effect of series and parallel combinations of piezoelectric harvesters on the output voltage of the piezoelectric has also been studied (Dayou & Wang, 2009).

Optimizing the output power has been investigated for different circuits (G. A. Rincón-Mora & S. Yang, 2016). Various electronic interfaces including classic, voltage doubler, Synchronous Charge Extraction (SCE), Synchronized Switch Harvesting on Inductor (SSHI) circuits have been investigated and compared regarding output power (Qiu, Jiang, Ji, & Zhu, 2009). Different electronic circuits have been studied for improving output power as well as bandwidth of a single piezoelectric (I. Lien et al., 2010), and an array of piezoelectric harvesters (I. C. Lien & Shu, 2012). The SSHI circuit is also investigated in a circuit with an active rectifier to boost a PZT piezoelectric energy harvester's output power (L. Wu, X. D. Do, S. G. Lee, & D. S. Ha, 2017). The parallel combination of an inductor and resistor has been studied as the load for the piezoelectric circuit to boost the output power of a hydraulic pressure energy harvester (HPEH) (E A Skow and K A Cunefare and,A.Erturk, 2014). A bias-flip rectifier is investigated to flip the voltage across the piezoelectric internal capacitor as well as discharging it to reduce the amount of charge losses and maximize the output power (Y. K. Ramadass & A. P. Chandrakasan, 2010). The rectifier in this case includes an inductor along with a switch, which is controlled to turn on/off the inductor based on the state of the current. A power conditioning circuit using inductors for increasing the voltage and rectifying the current of a piezoelectric stack energy harvester has been investigated (Skow, Leadenham, Cunefare, & Erturk, 2016).

This study aims to investigate a method to increase a piezoelectric-based energy harvester's output power by using inductance. Piezoelectric energy harvesters in contrast to other electrical power generators have inherent capacitive internal impedance (Ottman et al., 2002). Optimal power is obtained when the power source has no impedance. This is while the internal capacitance of the piezoelectric has a negative reactance. Using inductance to improve the energy harvesting circuit has been preliminarily investigated in both theory and experiment (Zargarani & Mahmoodi, 2016; Zargarani & Mahmoodi, 2017). This paper builds upon the preliminary results of (Zargarani & Mahmoodi, 2016; Zargarani & Mahmoodi, 2017) and completes the theory and experimentation. The inductance is utilized to produce a positive reactance to reduce this negative reactance, and therefore increases the output power of the piezoelectric energy harvester. To this end, four circuits are experimentally studied: Simple Resistive Load (SRL), Inductive Load (IL), Standard AC-DC, and Inductive AC-DC circuits. The results indicate that higher output power is provided by the IL circuit compared to the SRL. The Inductive AC-DC circuit also outperforms the traditional standard AC-DC circuit.

2. Method

2.1 Dynamic Modeling of the Energy Harvesting Circuits

In this section, the various electrical interfaces for energy harvesting are presented. The SRL, shown in Figure 1, is the first circuit studied in this paper, as it is the building block of other circuits. In an SRL circuit, the piezoelectric terminals are connected directly to the load resistor. The voltage produced by the piezoelectric harvester is considered to be sinusoidal. It is placed in a series connection with the internal impedance of the piezoelectric energy harvester (Zargarani & Mahmoodi, 2015). The general formula for the output power of the SRL circuit is:

$$P_{output} = \frac{V_O^2}{R_L} \tag{1}$$

where R_L is the load resistance, and the amplitude of the output voltage, Vo, is:

$$V_O = V_P \left| \frac{R_L}{R_L + \frac{1}{jC_P\omega}} \right| \tag{2}$$

where C_P is the internal capacitance of the piezoelectric harvester, V_P is the piezoelectric open circuit voltage, and ω is the system's excitation frequency. Output power is:

$$P_{output} = V_P^2 \frac{R_L (C_P \omega)^2}{1 + (R_L C_P \omega)^2} \tag{3}$$

The optimal resistance is found by setting to zero the derivative of the power, with respect to load resistance. The optimal load resistance is:

$$R_{optimal} = \frac{1}{C_P \omega} \tag{4}$$

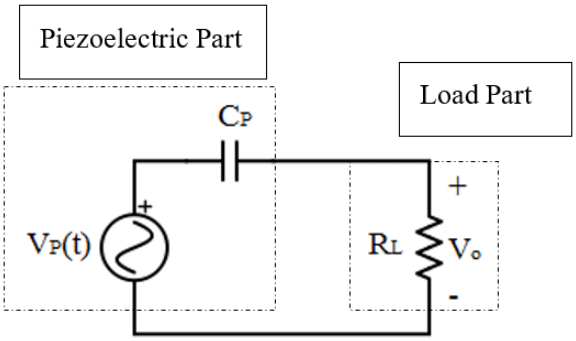

Figure 1. SRL circuit including the piezoelectric model (Zargarani & Mahmoodi, 2016)

An easier method for obtaining the optimal value of the load resistance is applying maximum power transfer theorem. Based on this theorem, output power of an electrical interface is maximum when the load impedance is equal to the complex conjugate of the source impedance at the frequency of excitation. In other words, when a circuit consists of resistive and (or) reactive electrical elements, maximum power is obtained when the resistance of the load equals that of the source, and the load reactance has the same magnitude but opposite sign as the source reactance at the frequency of excitation (Cartwright, 2008). This theorem presents an approach to choose the optimal load impedance based on the given source impedance, and not the opposite way. In fact, a source with zero impedance provides the maximum power transfer regardless of the impedance of the load. Thus, it is concluded that decreasing the source impedance can increase the output power.

The motivation for this investigation is obtaining optimal output power from a piezoelectric harvester. Piezoelectric harvesters include a capacitive impedance. Therefore, the new method of adopting inductance is proposed to reduce the internal reactance of the piezoelectric, and improve the output power. To this end, different values of inductance based upon the load resistance value and the system's excitation frequency should be utilized. This is discussed in details in this paper.

Maximum power transfer theorem states that obtaining maximum output power requires the impedance of the load to be equal to the source impedance's complex conjugate. Therefore:

$$Z_L = Z_S^* \tag{5}$$

where Z is the impedance, and L and S indices represent load and source, respectively. The complex forms of the load and source impedances are:

$$Z_L = R_L + jX_L \tag{6}$$

$$Z_S = R_S + jX_S \tag{7}$$

where R_i is the real component and X_i is the imaginary component of the impedance. For a SRL circuit, X_L is zero since the load impedance consists of only resistance. The value of R_S is also zero, for there is only a capacitive impedance on the piezoelectric harvester. Thus, the load resistance's optimal value equals the absolute value of the imaginary component of the source impedance:

$$|X_S| = \frac{1}{C_P \omega} \tag{8}$$

It is observed that the magnitude of the optimal load resistance is the same as the optimal resistance found in equation (4). This conclusion is valid only for the cases where the load impedance has to be purely resistive. However, in a general case where the load does not have to include only resistive components, inductive

components could be utilized in the circuit to improve the output power of the piezoelectric circuit. Therefore, a new electrical interface, IL circuit, is proposed and shown in Figure 2. The IL circuit has an inductor which is in series connection with the load resistance.

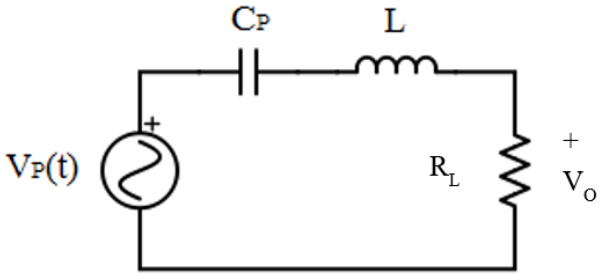

Figure 2. IL circuit schematic (Zargarani & Mahmoodi, 2016)

The optimal load resistance is obtained using equation (5). Substituting for source and load impedances using equations (6) and (7) yields to:

$$R_L + jX_L = R_S - jX_S \tag{9}$$

The source does not have any resistance, therefore:

$$R_L = \left| -j(X_L + X_S) \right| \tag{10}$$

where $X_L = L\omega$, L is the inductance of the load, and $X_S = -1/C_P\omega$. Thus, the optimal load resistance is:

$$R_{optimal} = \left| L\omega - \frac{1}{C_P\omega} \right| \tag{11}$$

This result shows that adding inductance to the electrical circuit reduces the optimal resistance by reducing the capacitive effect of the reactance of the source impedance. The IL circuit could also be interpreted such that the inductor is in a series connection with the capacitive impedance of the piezoelectric harvester. The decrease in the impedance of the source results in increase of the output power. Therefore, the IL circuit is supposed to outperform the SRL circuit regarding output power. However, it still provides AC voltage that requires to be rectified in order to be stored. Therefore, the Inductive AC-DC circuit is suggested such that it has the properties of both IL and the standard AC-DC circuits (Priya & Inman, 2009). It adopts an inductance to reduce the value of the internal capacitance of the piezoelectric as in the IL circuit, and also provides DC voltage as in the standard AC-DC circuit. The Inductive AC-DC circuit is made such that it has an inductor in the source side of the standard AC-DC circuit. The Inductive AC-DC circuit is then investigated experimentally to see the effect of adopting the inductive element on the output power. The standard AC-DC circuit is shown in Figure 3, and the Inductive AC-DC circuit is shown in Figure 4.

The standard AC-DC circuit is made of a full wave bridge rectifier, where its output is (J. Dicken, P. D. Mitcheson, I. Stoianov, & E. M. Yeatman, 2012):

$$P_{out} = \frac{2}{\Pi} I_P V_O \left| 1 - \frac{V_O + 2V_D}{V_P} \right| \tag{12}$$

where I_P represent the piezoelectric's current and V_D represents the voltage loss across each diode of the rectifier. The optimal output voltage is (J. Dicken et al., 2012):

$$V_{O,optimal} = \frac{1}{2}(V_P - 2V_D) \tag{13}$$

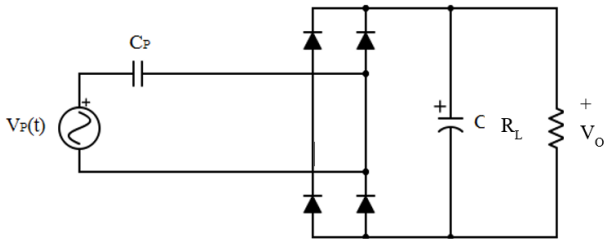

Figure 3. Standard AC-DC circuit schematic (Zargarani & Mahmoodi, 2016)

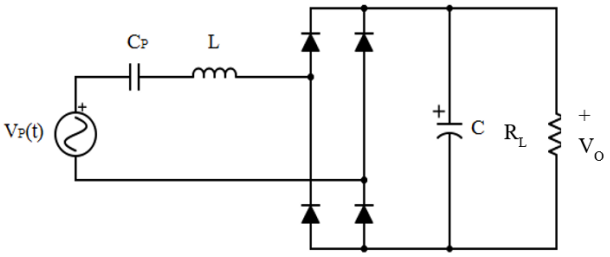

Figure 4. Inductive AC-DC circuit schematic (Zargarani & Mahmoodi, 2016; Zargarani & Mahmoodi, 2017)

The voltage drop across a diode, V_D, is assumed to be zero, as diodes are considered to be ideal. Therefore, the optimal output power is:

$$P_{optimal} = \frac{1}{2\Pi}\frac{{V_P}^2}{Z_P} \tag{14}$$

where Z_P is the piezoelectric impedance. Based on equation (14), the reduction of the source impedance enhances the output power. The internal impedance in the standard AC-DC circuit is equal to the capacitance of the source (piezoelectric), which is:

$$Z_P = \left|\frac{1}{jC_P\omega}\right| \tag{15}$$

The Inductive AC-DC circuit is made by adding an inductor in a series connection with the internal capacitance of the piezoelectric, before the diode bridge in the standard AC-DC circuit. Thus, the Inductive AC-DC circuit's internal impedance becomes:

$$Z_P = \left|j(L\omega - \frac{1}{C_P\omega})\right| \tag{16}$$

According to equation (16), increase in the amount of inductance reduces the amount of the impedance, which in turn boosts the output power according to equation (14). Nevertheless, the value of $L\omega$ should be less than $1/C_P\omega$.

2.2 Numerical Analysis of the Energy Harvesting Circuits

In this section, the numerical analysis to investigate the effect of the inductance on energy harvesting circuits is presented. The inductance is added to the SRL and standard AC-DC circuits to build the IL and Inductive AC-DC circuits, respectively. The piezoelectric harvester is assumed to be in the shape of a patch adhered to the surface of a cantilever beam. To compare the numerical with actual experimental results, the values of a real experimental study is used. The experimental study is discussed in the following section. The internal capacitance of the piezoelectric used in this research is found to be 56 nF. The first two resonant frequencies of the cantilever beam are 10.53 Hz and 62.7 Hz (Omidi, Mahmoodi, & Shepard Jr., 2015). The second resonant frequency of the beam is used in this research as the frequency of the excitation since the first resonant frequency of the cantilever beam does not provide sufficient output voltage in the linear vibration region. The first circuit investigated is the SRL

circuit. Figure 5 shows the variation of the output power of this circuit at 62.7 Hz based on the variation in the load resistance. It is observed in the figure that the optimal output power occurs at optimal resistance, whose value is 45328 Ω in this case. The optimal resistance is found to be dependent on the excitation frequency.

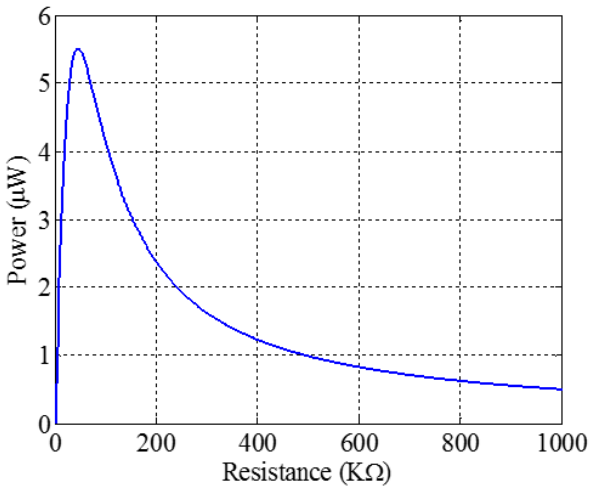

Figure 5. Variation of output power of SRL based on load resistance

The changes in the output power versus the load resistance at various frequencies of excitation with identical input voltage is shown in Figure 6. Increasing the frequency appears to increase the optimal output power and shift the optimal load resistance. However, increasing the input voltage to the circuit (piezoelectric output voltage), which is proportional to the amplitude of excitation applied to the piezoelectric, amplifies the output power without altering the optimal resistance. This is shown in Figure 7.

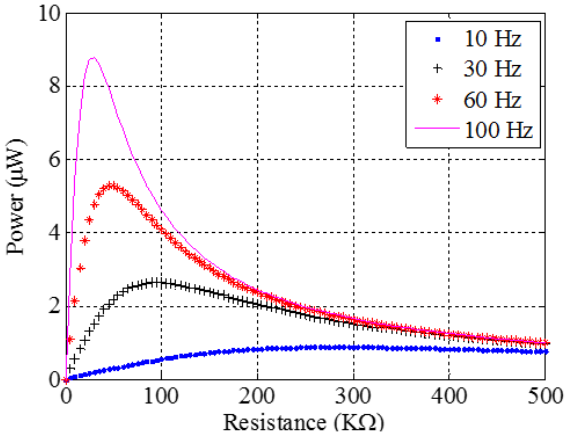

Figure 6. Output power of SRL at various frequencies (V_{in} = 1 V)

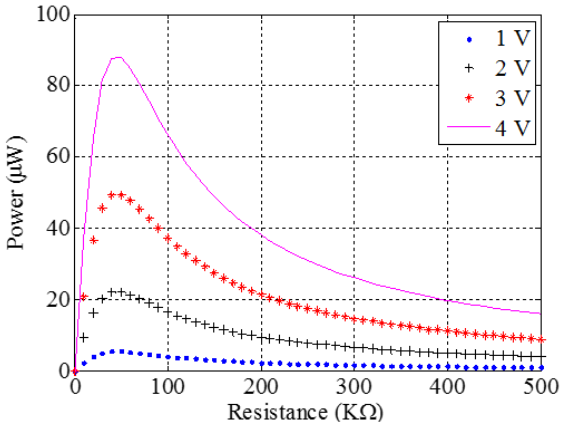

Figure 7. Output power of SRL at different input voltages (f = 62.7 Hz)

The next circuit studied numerically is the IL circuit. According to equation (11), optimal load resistance (inductance) depends on both source capacitance and inductance (load resistance). Therefore, the numerical analysis is performed with varying the load resistance and inductance simultaneously based on equation (11). It means that as the load resistance or inductance is increased, the other one must be decreased. This correlation for keeping the output power at optimal value is shown in Figure 8. The relation between the output power and inductance in Figure 9 shows that an increase in the value of the inductance (simultaneously with a decrease in the load resistance) increases the output power. Nevertheless, inductance values must be selected in a way that it has a smaller reactance value compared to the absolute value of the reactance of the piezoelectric internal capacitance.

Figure 9 and Table 1 show the maximum value of inductance that is employed in the numerical analysis and the corresponding output power.

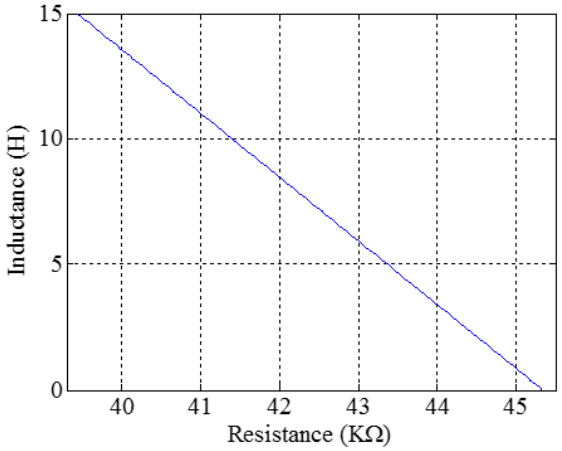

Figure 8. Simultaneous variation of inductance and resistance in IL circuit

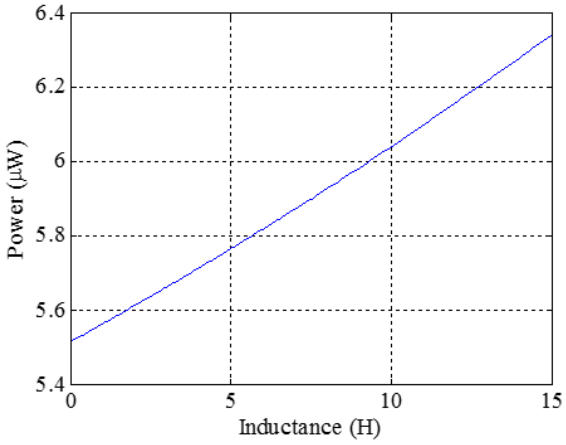

Figure 9. Variation of output power based on inductance in IL circuit

The variation in the output power versus the variation in the load resistance is shown in Figure 10. Increasing the load resistance is shown to reduce the output power. Nonetheless, the load resistance cannot reach zero, as shown in Figure 10, if it is desired to obtain active power. Thus, the least amount of resistance that is used for the IL circuit in this study is considered as the optimal load resistance, for it produces the maximum amount of output power compared to the other load resistances used in this research. Lastly, Figure 11 presents a 3D plot showing the variation in the output power based on both load resistance and inductance. The curve in this figure represents the optimal output power corresponding to the optimal resistance (inductance) for a given value of inductance (resistance) according to equation (11). It is observed that an increase in the amount of the inductance, while the load resistance is decreased according to equation (11), results in an increase in the output power.

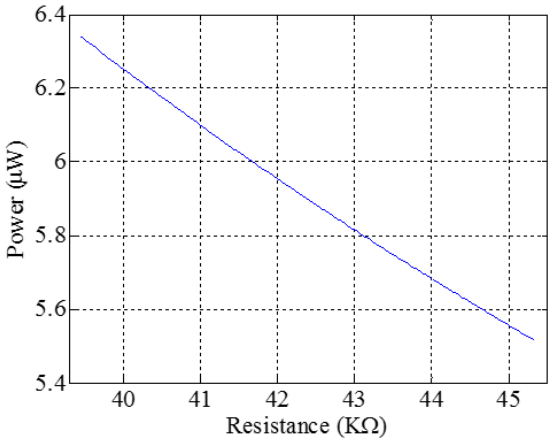

Figure 10. Variation of output power based on load resistance in IL circuit

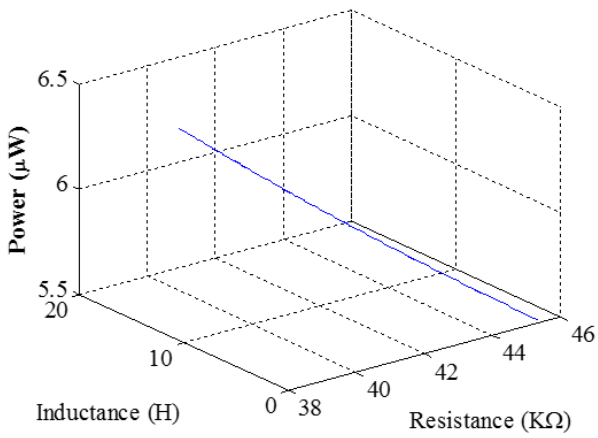

Figure 11. Variation of output power based on load resistance and inductance in IL circuit

The effect of increasing the amount of the inductance in the IL circuit is shown in Figure 12. The IL circuit with L=0 is the same as the SRL circuit. Increasing the value of inductance added to the circuit is observed to increase the optimal output power while it decreases the optimal resistance.

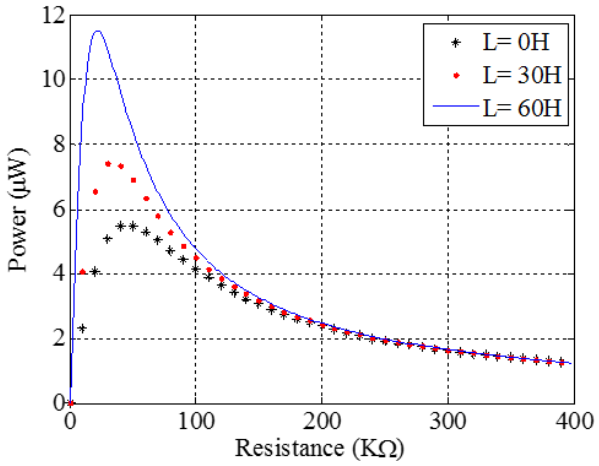

Figure 12. Variation of output power based on load resistance; the asterisks show the SRL circuit (L=0), while the dots and solid line show the IL circuit with 30, and 60 H inductors respectively

Table 1 presents the values of the optimal resistances found in the range of resistances investigated in this research for the SRL and IL circuits as well as their corresponding output powers. The IL circuit that adopts the larger amount of inductance is observed to produce higher output power compared to the SRL circuit.

Table 1. Optimal resistance and the corresponding power in the range used for SRL and IL circuits at 62.7 Hz.

	SRL Circuit	IL Circuit
Optimal Resistance (Ω)	45328	39418
Max Inductance (H)		15
Max Power (μW)	5.5154	6.3422

Finally, Figure 13 shows the variation of the output power of the Inductive AC-DC circuit based on the inductance while the input voltage (produced by the piezoelectric) is kept at 1 V, and the source impedance is changed with the change in inductance based on equation (16). The starting point of the plot in the figure corresponds to the standard AC-DC circuit as it does not have any amount of inductance (L=0). The output power is shown to increase with the increase in the amount of the inductance.

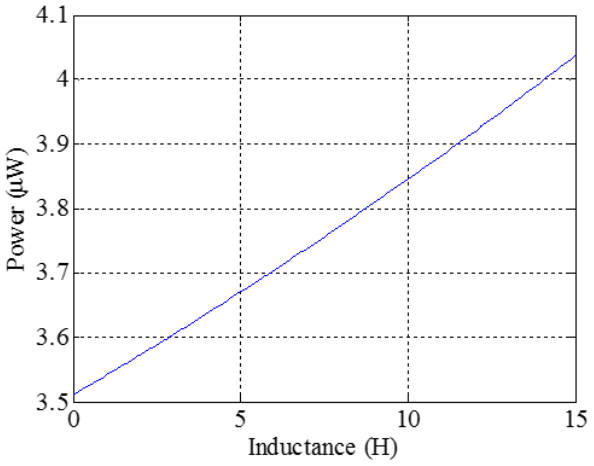

Figure 13. Variation of output power based on inductance in Inductive AC-DC circuit

2.3 Experimental Setup

In order to validate the result of the numerical study, a set of experiments is tested and presented in this section. A piezoelectric ceramic made by Piezo Systems, Inc.®, is used with properties as given in Table 2. The piezoelectric patch is attached on an aluminum cantilever beam using epoxy (Omidi et al., 2015) as shown in Figure 14. The cantilever beam properties are given in Table 3. The clamped end of the cantilever beam is attached to a shaker and the piezoelectric is attached on the beam such that its midpoint is 76 mm apart from the clamped base of the cantilever beam. It should be attached close to the base for maximum energy harvesting; however, it could not be attached too close due to experimental limitations. In order to produce the input signal for the shaker, a model AFG3022B function generator built by Tektronix Inc.® is utilized. However, the input signal first has to be amplified, which is accomplished by utilizing an amplifier built by Labworks Inc. ®.

Table 2. Properties of the piezoelectric.

Description	Length (mm)	Width (mm)	Thickness (mm)	Capacitance (nF)
Value	31.75	12.70	0.5	56

Table 3. Properties of the cantilever beam.

Description	Length (mm)	Width (mm)	Thickness (mm)	Density (Kg/m^3)	Young's Modulus (GPa)
Value	325.20	12.70	1.58	2710	70

As mentioned in the previous section, the second natural frequency of the beam is used as the excitation frequency. Therefore, the beam is excited at the frequency of 62.7 Hz in all the experiments in this research. There are four electrical circuits investigated experimentally: SRL, IL, standard AC-DC, and Inductive AC-DC circuits.

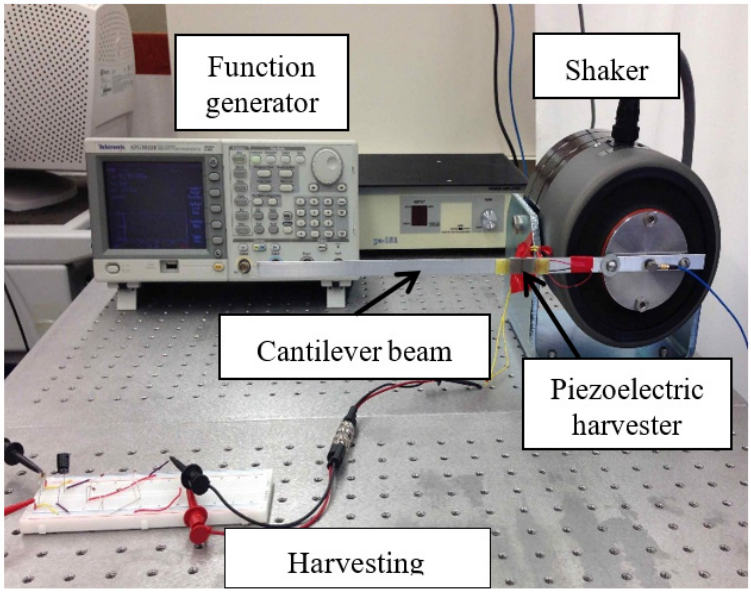

Figure 14. Experimental setup for the piezoelectric harvester attached on the cantilever beam (Zargarani & Mahmoodi, 2017)

The first experiment utilized the SRL circuit in order to experimentally find the value of the optimal load resistance. The internal capacitance of the piezoelectric is then calculated based on equation (4). For this purpose, the SRL circuit is made by connecting the output electrodes of the piezoelectric directly to a variety of different values of resistances. The output voltage is measured and recorded via oscilloscope. The experiment is performed three times in order to validate the result.

The next experiment is performed on the IL circuit for different amounts of inductors based on our accessible facilities: 1, 4.7 and 10 mH. Each value of inductor is tested with various load resistances ranging from 22 KΩ to 1 MΩ. Afterwards, an experiment is performed on the SRL circuit and the IL circuit that uses an inductor value of

10 mH. This experiment is performed on a smaller range of resistance values about the numerical optimal resistance. Then, the experiments on the standard AC-DC and the inductive AC-DC circuits are performed. The standard AC-DC circuit is composed of a full wave diode rectifier, a filter capacitor, and a load resistor. A filter capacitor with the value of 100 μF is used to decrease the amount of the ripple voltage and smoothen the output voltage (Hambley, 2005). The output power of the piezoelectric harvester is small, therefore, it is important to choose diodes with low voltage drop. The 1N3064 diodes are used to construct the full wave diode rectifier as they have low voltage drop. Then various amounts of resistances are connected in a parallel combination with the filter capacitor. The output voltages across the load resistors are recorded via oscilloscope. In the next step, the Inductive AC-DC circuit is tested. This circuit is identical to the standard AC-DC circuit except that it utilizes an inductor before the rectifier bridge. The same inductors as in the experiment on the IL circuit are used for this experiment. Similarly, the same filter capacitor, load resistances, and input voltage are used in the experiments for both the standard AC-DC and Inductive AC-DC in order for their result to be comparable. Figure 15 shows the experimental set up used to run tests on the Inductive AC-DC circuit.

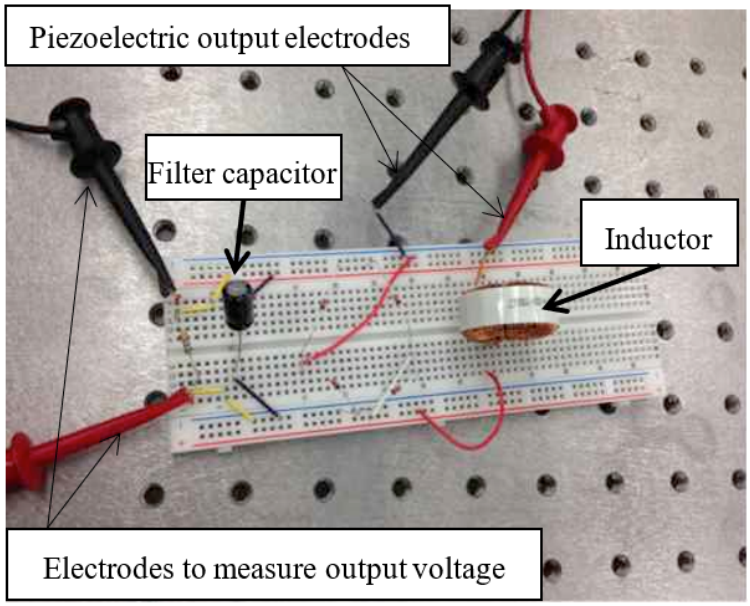

Figure 15. Experimental setup of Inductive AC-DC circuit (Zargarani & Mahmoodi, 2017)

3. Results

In this section, the results of the experiments to investigate the effect of adding inductance to the circuits is presented and compared with the numerical results. To validate the numerical results, the comparison between experimental and analytical data is performed in two stages. First, the resistance value that maximizes the power is validated, then the power vs. resistance curve is validated. This is due to the fact that the increments of change in resistance to find the maximum power are much smaller than the increments for the expanded curve. As described, the first experiment was run to find the value of the optimal load resistance, which was realized to be within 47 KΩ to 51 KΩ. Consequently, this range is focused on for finding the optimal resistance more accurately. This region of the power-resistance curve around the optimal resistance is shown in Figure 16. The uncertainty of the resistors and the measurement lead us to picking four points in this region. The optimal resistance is observed, from curve fitting, to be about 48.5 KΩ. This shows only 7% error compared to 45 KΩ (as in the numerical analysis) when it is connected in parallel with the resistance of the oscilloscope. This error in the value of the optimal resistance is because of connecting the load resistance to the oscilloscope, which has a resistance of about 1 MΩ. The parallel connection of the internal resistance of the oscilloscope and the load resistance where the power is optimal, is about 45 KΩ. Using this value for the optimal resistance in equation (4), the internal capacitance of the piezoelectric patch is determined to be 56 nF. This value is used throughout this study for the internal capacitance.

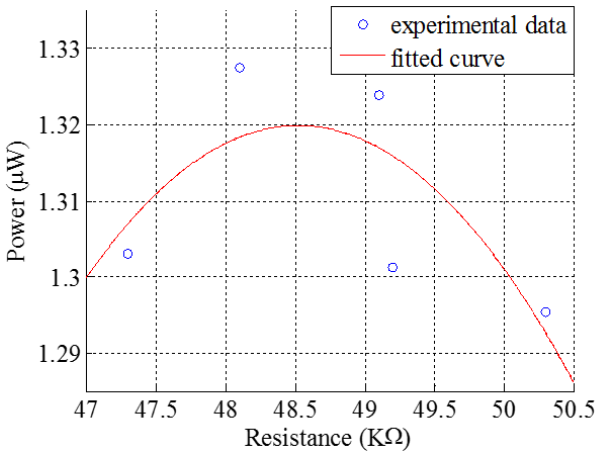

Figure 16. Variation of output power based on load resistance (SRL); circles represent the experimental data points, while the solid line indicates the fitted curve (Zargarani & Mahmoodi, 2017)

The graphs in Figures 17-20 show the comparison of the experimental results with the numerical results for the SRL and the IL circuits. These graphs are based on the load resistance connected to the oscilloscope. Connecting the load resistance in parallel with the oscilloscope's resistance results in decreasing the total value of the load resistance. Consequently, the range used for the load resistance, as mentioned in the previous section, changes (from 22KΩ-1MΩ) to 21 KΩ to 476 KΩ as they are connected to the circuit. The experimental results verify the numerical results. The small changes in the optimal resistances are smaller than the resistor error. Therefore, the experimental optimal resistance for all four cases is kept constant for all inductor values utilized in the experiment. The numerical graphs in this section are based on the chosen experimental resistor and inductor values. Therefore, the numerical optimal resistance utilized in the experiments is not expected to vary drastically, with only a slight decrease in the optimal resistance as the inductance is increased. Consequently, the peak values in the numerical graphs are shifted very slightly. The numerical results and the experimental results are found to be in good compatibility based on the inductor values utilized in the experiments.

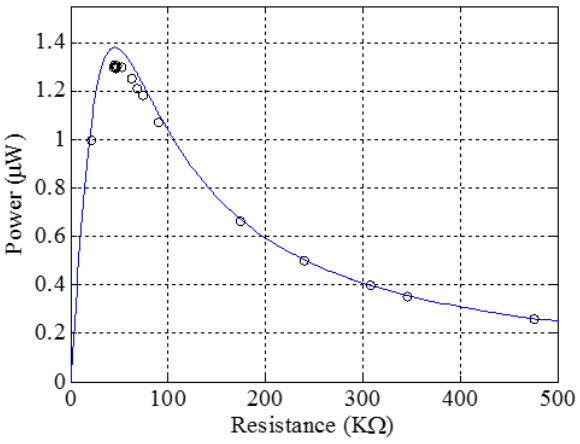

Figure 17. Variation of output power based on load resistance in SRL (L=0 mH). The solid line and circles show the numerical and experimental results respectively

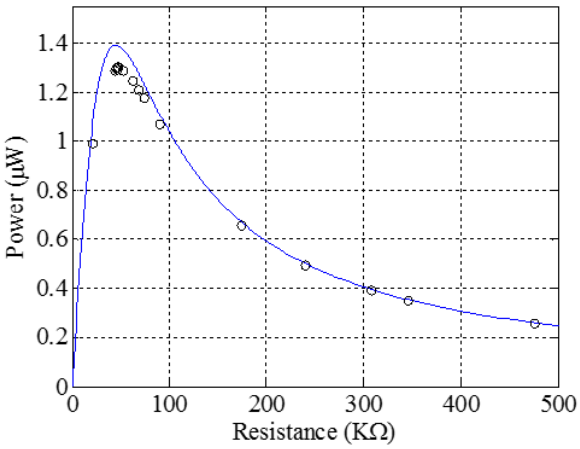

Figure 18. Variation of output power based on load resistance in IL circuit (L=1 mH). The solid line and circles show the numerical and experimental results respectively

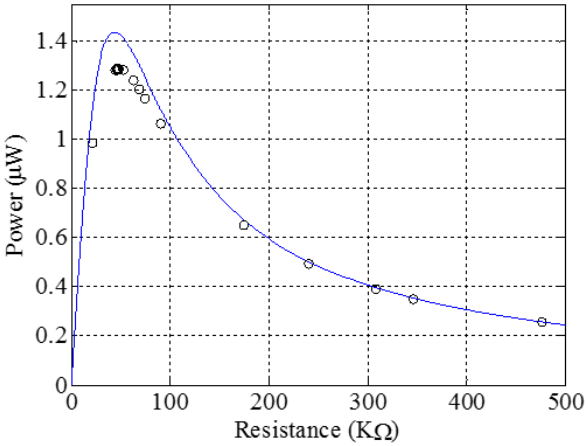

Figure 19. Variation of output power based on load resistance in IL circuit (L=4.5 mH). The solid line and circles show the numerical and experimental results respectively

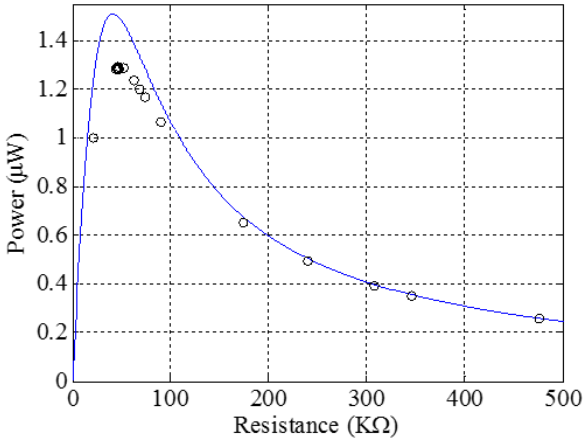

Figure 20. Variation of output power based on load resistance, IL circuit (L=10 mH). The solid line and circles show the numerical and experimental results respectively (Zargarani & Mahmoodi, 2017)

To show the effect of the inductance in circuits more clearly, the result of an experiment on only the SRL circuit and the IL circuit with 10 mH inductor over a smaller range of resistance is shown in Figure 21. This plot includes only the load resistances that have higher output power in comparison to other load resistances in order to show the difference between output powers of the SRL and IL circuits more clearly. The 10 mH inductor is observed to increase the output power by 0.24% in comparison to the SRL circuit that does not utilize any inductance. The optimal load resistance is observed to be 48 KΩ. Since the range for the output power in these experimental tests is small, a slight amount of noise may result in changing the results.

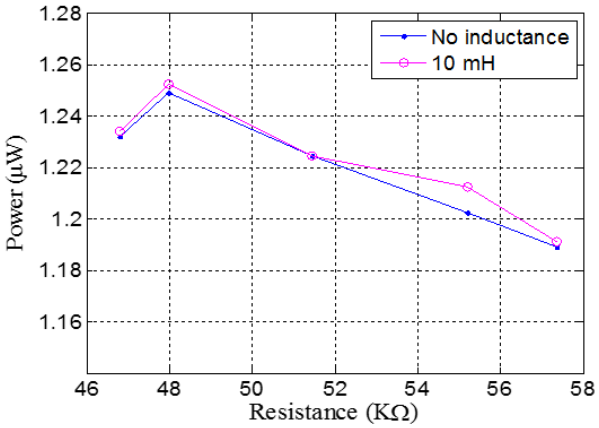

Figure 21. Variation of output power based on load resistance in SRL and IL circuit with L=10 mH (Zargarani & Mahmoodi, 2017)

In order to obtain DC voltage output, a full wave bridge rectifier (standard AC-DC circuit) was utilized. Then, an Inductive AC-DC circuit was built by adding an inductor to the traditional standard AC-DC circuit. The Inductive AC-DC circuit was investigated for different values of the inductance, and is compared with the standard AC-DC circuit. The experimental results for output power of both standard and Inductive AC-DC circuits are shown in Figure 22. The range of values used for load resistances is selected in a way so that only the values that have higher output powers are compared. According to the figure, increasing the inductance value increases the output power. In order to show the effect of the added inductance more clearly, the output power of both the standard AC-DC circuit and Inductive AC-DC circuit with 10 mH inductor are compared in Figure 23. The Inductive AC-DC circuit is observed to enhance the output power by 6.7% compared to the standard AC-DC circuit. Such result was expected since adding inductance decreases the source impedance as stated in equation (16) and the reduction of source impedance increases the output power as stated in equation (14).

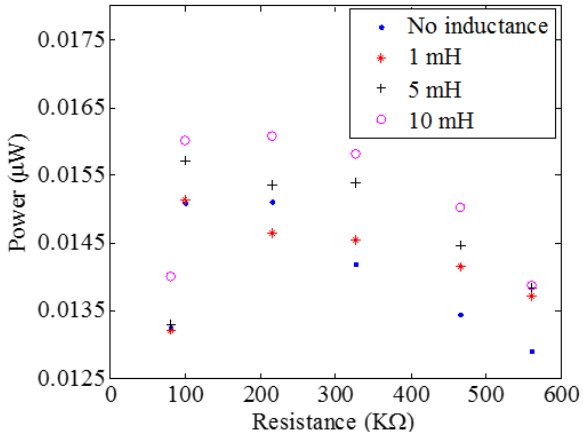

Figure 22. Variation of output power based on load resistance in standard AC-DC and Inductive AC-DC

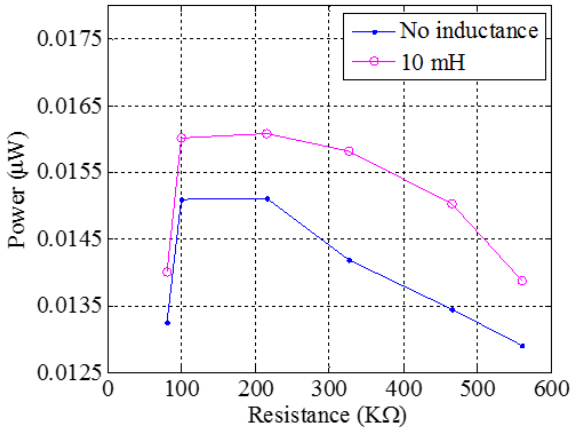

Figure 23. Variation of output power based on load Resistance in standard AC-DC and Inductive AC-DC (L=10 mH) (Zargarani & Mahmoodi, 2017)

4. Conclusion

A new method for improving the output power of a piezoelectric vibration energy harvester was investigated analytically and verified experimentally. The new approach utilized inductance to decrease the internal reactance of the piezoelectric harvester, and hence, improve the output power. For this purpose, four electrical interfaces were tested experimentally for a beam piezoelectric harvester; SRL, IL, standard AC-DC, and Inductive AC-DC circuits. The IL circuit shows to improve the output power compared to the SRL. Furthermore, the inductive AC-DC circuit shows 6.7% increase in the output power compared to the standard AC-DC circuit. It is concluded that increasing the value of inductance simultaneously while reducing the value of the resistance increases the output power in both IL and Inductive AC-DC circuits. The increase in the value of the inductor causes the size of the circuit to expand. Consequently, it makes the circuit impractical for applications that require the circuit move with the source of vibration. It can still be employed in applications that do not require the circuit move with the energy harvester. Nevertheless, the values used for the inductance do not surpass the maximum value as found based on the load resistance and the piezoelectric internal capacitance at the excitation frequency. Furthermore, the load resistance cannot be eliminated as active output power is desired.

References

Baldwin, J. D., Roswurm, S., Nolan, J., & Holliday, L. (2011). *Energy Harvesting on Highway Bridges.*

Cartwright, K. V. (2008). Non-calculus derivation of the maximum power transfer theorem. *The Technology Interface/Spring.*

Choi, D., Han, C., Kim, H., & Yoon, J. (2011). Liquid-based electrostatic energy harvester with high sensitivity to human physical motion. *Smart Materials and Structures, 20*(12), 125012. https://doi.org/10.1088/0964-1726/20/12/125012

Dayou, J., & Wang, S. (2009). Generating electricity using piezoelectric material.

De Pasquale, G., & Soma, A. (2013). Energy harvesting from human motion with piezo fibers for the body monitoring by MEMS sensors. Paper presented at the *Design, Test, Integration and Packaging of MEMS/MOEMS (DTIP), 2013 Symposium On,* 1-6.

Skow, E. A., Cunefare, K. A., & Erturk, A. (2014). Power performance improvements for high pressure ripple energy harvesting. *Smart Materials and Structures, 23*(10), 104011. https://doi.org/10.1088/0964-1726/23/10/104011

Erturk, A., & Inman, D. J. (2008). On mechanical modeling of cantilevered piezoelectric vibration energy harvesters. *Journal of Intelligent Material Systems and Structures,* https://doi.org/10.1177/1045389X07085639

Frey, G., Carmichael, B., Kavanaugh, J., & Mahmoodi, S. N. (2014). Dynamic model and simulation of flag vibrations modeled as a membrane. Paper presented at the *ASME 2014 Dynamic Systems and Control Conference,* V003T53A001-V003T53A001. https://doi.org/10.1115/DSCC2014-5897

Fröhlich, A. A., Bezerra, E. A., & Slongo, L. K. (2014). Experimental analysis of solar energy harvesting circuits efficiency for low power applications. *Computers & Electrical Engineering,* https://doi.org/10.1016/j.compeleceng.2014.09.004

Rincón-Mora, G. A., & Yang, S. (2016). Tiny piezoelectric harvesters: Principles, constraints, and power conversion. *IEEE Transactions on Circuits and Systems I: Regular Papers, 63*(5), 639-649. https://doi.org/10.1109/TCSI.2016.2555249

Hadas, Z., Kluge, M., Singule, V., & Ondrusek, C. (2007). Electromagnetic vibration power generator. Paper presented at the *Diagnostics for Electric Machines, Power Electronics and Drives, 2007. SDEMPED 2007. IEEE International Symposium On,* 451-455. https://doi.org/10.1109/DEMPED.2007.4393136

Hambley, A., R. (2005). Rectifier circuits. *Electrical engineering principles and applications* (3rd ed.,) Pearson Prentice Hall.

Hatti, N., Tungpimolrut, K., Phontip, J., Pechrach, K., Manoonpong, P., & Komol, K. (2011). A PZT modeling for energy harvesting circuits. Paper presented at the *Applications of Ferroelectrics (ISAF/PFM), 2011 International Symposium on and 2011 International Symposium on Piezoresponse Force Microscopy and Nanoscale Phenomena in Polar Materials,* 1-4. https://doi.org/10.1109/ISAF.2011.6014127

Li, H. Y., Li, H., & Tzou, H. S. (2011). A circuit design in piezoelectric vibration measurement system. Paper presented at the *Piezoelectricity, Acoustic Waves and Device Applications (SPAWDA), 2011 Symposium On,* 532-535. https://doi.org/10.1109/SPAWDA.2011.6167306

Dicken, J., Mitcheson, P. D., Stoianov, I., & Yeatman, E. M. (2012). Power-extraction circuits for piezoelectric energy harvesters in miniature and low-power applications. *IEEE Transactions on Power Electronics, 27*(11), 4514-4529. https://doi.org/10.1109/TPEL.2012.2192291

Ju, S., Chae, S. H., Choi, Y., Jun, S., Park, S. M., Lee, S., . . . Ji, C. (2013). Harvesting energy from low frequency vibration using MSMA/MFC laminate composite. Paper presented at the *Solid-State Sensors, Actuators and Microsystems (TRANSDUCERS & EUROSENSORS XXVII), 2013 Transducers & Eurosensors XXVII: The 17th International Conference On,* 1348-1351. https://doi.org/10.1109/Transducers.2013.6627027

Kodali, P., Mahidhar, M. N., Lokesh, N., Prasad, M. V. N., & Sambandan, S. (2012). Vibration energy harvesting. Paper presented at the *Emerging Electronics (ICEE), 2012 International Conference On,* 1-4. https://doi.org/10.1109/ICEmElec.2012.6636258

Korayem, M. H., & Omidi, E. (2012). Robust controlled manipulation of nanoparticles using atomic force microscope. *Micro & Nano Letters, IET, 7*(9), 927-931. https://doi.org/10.1049/mnl.2012.0293

Wu, L., Do, X. D., Lee, S. G., & Ha, D. S. (2017). A self-powered and optimal SSHI circuit integrated with an active rectifier for piezoelectric energy harvesting. *IEEE Transactions on Circuits and Systems I: Regular Papers, 64*(3), 537-549. https://doi.org/10.1109/TCSI.2016.2608999

Lien, I. C., & Shu, Y. C. (2012). Array of piezoelectric energy harvesting by the equivalent impedance approach. *Smart Materials and Structures, 21*(8), 082001 (8 pp.). https://doi.org/10.1088/0964-1726/21/8/082001

Lien, I., Shu, Y., Wu, W., Shiu, S., & Lin, H. (2010). Revisit of series-SSHI with comparisons to other interfacing circuits in piezoelectric energy harvesting. *Smart Materials and Structures, 19*(12), 125009. https://doi.org/10.1088/0964-1726/19/12/125009

Monfray, S., Puscasu, O., Savelli, G., Soupremanien, U., Ollier, E., Guerin, C., … Skotnicki, T. (2012). Innovative thermal energy harvesting for zero power electronics. Paper presented at the *Silicon Nanoelectronics Workshop (SNW), 2012 IEEE,* 1-4. https://doi.org/10.1109/SNW.2012.6243313

Niotaki, K., Georgiadis, A., & Collado, A. (2013). Thermal energy harvesting for power amplifiers. Paper presented at the *Radio and Wireless Symposium (RWS), 2013 IEEE,* 196-198. https://doi.org/10.1109/RWS.2013.6486686

Nuffer, J., & Bein, T. (2006). Applications of piezoelectric materials in transportation industry. Paper presented at the *Proceedings of Global Symposium on Innovative Solutions for the Advancement of the Transport Industry, San Sebastian, Spain,*

Omidi, E., Korayem, A. H., & Korayem, M. H. (2013). Sensitivity analysis of nanoparticles pushing manipulation by AFM in a robust controlled process. *Precision Engineering, 37*(3), 658-670. https://doi.org/10.1016/j.precisioneng.2013.01.011

Omidi, E., Mahmoodi, S. N., & Shepard Jr., W. S. (2015). Vibration reduction in aerospace structures via an

optimized modified positive velocity feedback control. *Aerospace Science and Technology, 45*, 408-415. https://doi.org/10.1016/j.ast.2015.06.012

Ottman, G. K., Hofmann, H. F., Bhatt, A. C., & Lesieutre, G. A. (2002). Adaptive piezoelectric energy harvesting circuit for wireless remote power supply. *Power Electronics, IEEE Transactions On, 17*(5), 669-676. https://doi.org/10.1109/TPEL.2002.802194

Peigney, M., & Siegert, D. (2013). Piezoelectric energy harvesting from traffic-induced bridge vibrations. *Smart Materials and Structures, 22*(9), 095019. https://doi.org/10.1088/0964-1726/22/9/095019

Priya, S., & Inman, D. J. (2009). *Energy harvesting technologies* Springer.

Qiu, J., Jiang, H., Ji, H., & Zhu, K. (2009). Comparison between four piezoelectric energy harvesting circuits. *Frontiers of Mechanical Engineering in China, 4*(2), 153-9. https://doi.org/10.1007/s11465-009-0031-z

Roundy, S., Wright, P. K., & Rabaey, J. (2003). A study of low level vibrations as a power source for wireless sensor nodes. *Computer Communications, 26*, 1131-1144. https://doi.org/10.1016/S0140-3664(02)00248-7

Skow, E., Leadenham, S., Cunefare, K. A., & Erturk, A. (2016). Power conditioning for low-voltage piezoelectric stack energy harvesters. Paper presented at 97990P-9799-9. Retrieved from http://dx.doi.org/10.1117/12.2219211

Sodano, H. A., Inman, D. J., & Park, G. (2005a). Comparison of piezoelectric energy harvesting devices for recharging batteries. *Journal of Intelligent Material Systems and Structures, 16*(10), 799-807. https://doi.org/10.1177/1045389X05056681

Sodano, H. A., Inman, D. J., & Park, G. (2005b). Generation and storage of electricity from power harvesting devices. *Journal of Intelligent Material Systems and Structures, 16*(1), 67-75. https://doi.org/10.1177/1045389X05047210

Wang, Q., Sun, C., & Qin, L. (2008). Piezoelectric energy harvesting using single crystal pb (Mg1/3Nb2/3) O3-xPbTiO3 (PMN-PT) device. *Journal of Intelligent Material Systems and Structures,* https://doi.org/10.1177/1045389X08097385

Wynn, L. T., Truitt, A., Heim, I., & Mahmoodi, S. N. (2013). Modeling and response analysis of piezoelectric flag in wind flow. Paper presented at the *ASME 2013 Dynamic Systems and Control Conference,* V001T03A001-V001T03A001. https://doi.org/10.1115/DSCC2013-3912

Xu, T., Siochi, E. J., Kang, J. H., Zuo, L., Zhou, W., Tang, X., & Jiang, X. (2013). Energy harvesting using a PZT ceramic multilayer stack. *Smart Materials and Structures, 22*(6), 065015. https://doi.org/10.1088/0964-1726/22/6/065015

Ramadass, Y. K., & Chandrakasan, A. P. (2010). An efficient piezoelectric energy harvesting interface circuit using a bias-flip rectifier and shared inductor. *IEEE Journal of Solid-State Circuits, 45*(1), 189-204. https://doi.org/10.1109/JSSC.2009.2034442

Zargarani, A., & Mahmoodi, N. (2015). Investigating piezoelectric energy harvesting circuits for piezoelectric flags. Paper presented at the *ASME 2015 Conference on Smart Materials, Adaptive Structures and Intelligent Systems,* V002T04A014-V002T04A014. https://doi.org/10.1115/SMASIS2015-9011

Zargarani, A., & Mahmoodi, S. N. (2016). Enhancing the output power of a piezoelectric energy harvester by reducing the effect of the internal capacitance using inductance. Paper presented at the *ASME 2016 Conference on Smart Materials, Adaptive Structures and Intelligent Systems,* V002T07A014-V002T07A014. https://doi.org/10.1115/SMASIS2016-9288

Zargarani, A., & Mahmoodi, S. N. (2017). *Experimental investigation for enhancing the output power of a piezoelectric energy harvester*. https://doi.org/10.1115/SMASIS2017-3741

Zhao, J., & You, Z. (2014). A shoe-embedded piezoelectric energy harvester for wearable sensors. *Sensors, 14*(7), 12497-12510. https://doi.org/10.3390/s140712497